

# Effect of Gas Flow Rate and Gas Composition in Ar/CH<sub>4</sub> Inductively Coupled Plasmas

Lizhu Tong<sup>1</sup>

<sup>1</sup>Kesoku Engineering System Co., Ltd.

1-9-5 Uchikanda, Chiyoda-ku, Tokyo 101-0047, Japan, tong@kesco.co.jp

**Abstract:** The discharge properties in low pressure inductively coupled Ar/CH<sub>4</sub> plasmas operating at a rf frequency of 13.56 MHz and total gas pressure of 20 mTorr are studied in this work. The calculation of gas flow is performed in coupling with the plasma simulation. The gas flow rate is varied from 20 to 1000 sccm. The species taken into account include electrons, six kinds of molecules, eleven kinds of ions, five kinds of neutral radicals, and five kinds of excited species. 59 chemical reactions are considered. The density profiles of all the plasma species for the different gas flow rates and Ar fractions are obtained and the electron temperature and the total collisional power loss are presented.

**Keywords:** ICP plasma, Gas composition, Gas flow rate, Coupled calculation.

## 1. Introduction

Plasma-induced chemical-vapor deposition (PCVD) is the most common method used for the deposition of carbon films. One of the essential parameters to determine the PCVD growth of carbon film is the feed gases, such as CH<sub>4</sub>. Inductively coupled plasma (ICP) reactors which have high input efficiency and operate under lower gas pressure have been developed for microelectronics fabrication. The ICP plasmas are typically operated at pressures lower than 100 mTorr in typical electron density range of  $10^{16}$ - $10^{18}$  m<sup>-3</sup>. Such high-density plasmas containing CH<sub>4</sub> are useful sources of active species, such as dominant radicals like CH<sub>3</sub>, CH<sub>2</sub> and H for deposition [1-6].

The investigations of inductively coupled plasma discharges in CH<sub>4</sub> and its mixtures have been reported [1,7]. Bera and co-workers [1] used a self-consistent two-dimensional fluid model to study inductively coupled radio-frequency (13.56MHz) plasma discharges in CH<sub>4</sub> and a surface chemistry model was used to predict the diamond-like-carbon thin-film deposition/etch rate. Denysenko and co-workers

[7] studied the low-temperature deposition of ordered carbon nanostructures in inductively coupled Ar/CH<sub>4</sub>/H<sub>2</sub> plasmas by experiments and a spatially averaged (global) model, in which a low-frequency (0.46 MHz) ICP source was used. In their report, the densities of neutral and charged species were presented and the effect of Ar dilution and input flux of CH<sub>4</sub> in a range of flow rate of 3-8 sccm was discussed. Unfortunately, their study did not reveal the spatial profiles of neutral and charged species as well as the profiles of electron temperature and collisional power loss in the discharges, which are essential properties in low-temperature plasma discharges.

In this work, the inductively coupled rf (13.56 MHz) plasmas in Ar/CH<sub>4</sub> are studied by using an axisymmetrical two-dimensional fluid model provided in the Plasma Module of COMSOL Multiphysics. The plasma simulation is coupled with the solution of fluid dynamics. The discharge properties including the spatial profiles of all the plasma species as well as electron temperature and collisional power loss are reported. The effect of gas flow rate and gas composition in Ar/CH<sub>4</sub> on discharge properties is presented.

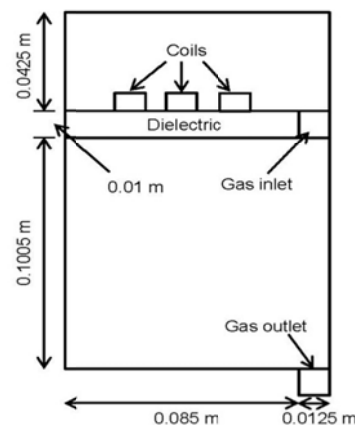


**Figure 1.** Model geometry used in this work.

## 2. Numerical Model

The model geometry used in this work is shown in Fig. 1, which has been described in earlier publications [8,9]. The simulations are performed for the case of Ar/CH<sub>4</sub> ICP plasma discharges operating at the rf frequency of 13.56 MHz and total gas pressure of 20 mTorr with the gas flow rates of 20-1000 sccm. The gas temperature is assumed to be 300 K and input power is 300 W. The Ar fractions in the Ar/CH<sub>4</sub>

**Table 1:** The electron reactions included in the model.

No.	Reaction	Ref.
1	$\text{Ar} + e^- \rightarrow \text{Ar}^* + e^-$	10
2	$\text{Ar}^* + e^- \rightarrow \text{Ar} + e^-$	10
3	$\text{Ar} + e^- \rightarrow \text{Ar}^+ + 2e^-$	10
4	$\text{Ar}^* + e^- \rightarrow \text{Ar}^+ + 2e^-$	10
5	$\text{CH}_4 + e^- \rightarrow \text{CH}_4^* + e^- (2 \text{ vib.})$	11
6	$\text{CH}_4 + e^- \rightarrow \text{CH}_4^+ + 2e^-$	11
7	$\text{CH}_4 + e^- \rightarrow \text{CH}_3^+ + \text{H} + 2e^-$	11
8	$\text{CH}_4 + e^- \rightarrow \text{CH}_3 + \text{H} + e^-$	11
9	$\text{CH}_4 + e^- \rightarrow \text{CH}_2 + 2\text{H} + e^-$	11
10	$\text{CH}_4 + e^- \rightarrow \text{CH} + 3\text{H} + e^-$	11
11	$\text{CH}_4 + e^- \rightarrow \text{CH} + 3\text{H} + e^-$	11
12	$\text{H}_2 + e^- \rightarrow \text{H}_2^+ + 2e^-$	12
13	$\text{H}_2 + e^- \rightarrow 2\text{H} + e^-$	12
14	$\text{H} + e^- \rightarrow \text{H}(2p, 3p) + e^-$	13
15	$\text{H}(2p, 3p) + e^- \rightarrow \text{H} + e^-$	13
16	$\text{H} + e^- \rightarrow \text{H}^+ + 2e^-$	13
17	$\text{C}_2\text{H}_2 + e^- \rightarrow \text{C}_2\text{H}_2^+ + 2e^-$	14
18	$\text{C}_2\text{H}_4 + e^- \rightarrow \text{C}_2\text{H}_2 + 2\text{H} + e^-$	14
19	$\text{C}_2\text{H}_4 + e^- \rightarrow \text{C}_2\text{H}_4^+ + 2e^-$	14
20	$\text{C}_2\text{H}_5 + e^- \rightarrow \text{C}_2\text{H}_4 + \text{H} + e^-$	14
21	$\text{C}_2\text{H}_5 + e^- \rightarrow \text{C}_2\text{H}_5^+ + 2e^-$	14
22	$\text{C}_2\text{H}_5 + e^- \rightarrow \text{C}_2\text{H}_4^+ + \text{H} + 2e^-$	14
23	$\text{C}_2\text{H}_6 + e^- \rightarrow \text{C}_2\text{H}_5 + \text{H} + e^-$	14
24	$\text{C}_2\text{H}_6 + e^- \rightarrow \text{C}_2\text{H}_4 + 2\text{H} + e^-$	14
25	$\text{C}_2\text{H}_6 + e^- \rightarrow \text{C}_2\text{H}_6^+ + 2e^-$	14
26	$\text{C}_2\text{H}_6 + e^- \rightarrow \text{C}_2\text{H}_5^+ + \text{H} + 2e^-$	14
27	$\text{CH}_3 + e^- \rightarrow \text{CH}_2 + \text{H} + e^-$	14
28	$\text{CH}_3 + e^- \rightarrow \text{CH} + 2\text{H} + e^-$	14
29	$\text{CH}_3 + e^- \rightarrow \text{CH}_3^+ + 2e^-$	14
30	$\text{CH}_2 + e^- \rightarrow \text{CH} + \text{H} + e^-$	14
31	$\text{CH}_2 + e^- \rightarrow \text{CH}_2^+ + 2e^-$	14
32	$\text{CH} + e^- \rightarrow \text{CH}^+ + 2e^-$	14
33	$\text{ArH}^+ + e^- \rightarrow \text{Ar} + \text{H}$	15

mixtures are varied from 0 to 100%. The species taken into account include electrons, atoms (Ar), molecules (H<sub>2</sub>, CH<sub>4</sub>, C<sub>2</sub>H<sub>2</sub>, C<sub>2</sub>H<sub>4</sub>, C<sub>2</sub>H<sub>6</sub>, C<sub>3</sub>H<sub>8</sub>), ions (Ar<sup>+</sup>, H<sub>2</sub><sup>+</sup>, H<sup>+</sup>, CH<sup>+</sup>, CH<sub>2</sub><sup>+</sup>, CH<sub>3</sub><sup>+</sup>, CH<sub>4</sub><sup>+</sup>, CH<sub>5</sub><sup>+</sup>, C<sub>2</sub>H<sub>2</sub><sup>+</sup>, C<sub>2</sub>H<sub>4</sub><sup>+</sup>, C<sub>2</sub>H<sub>5</sub><sup>+</sup>, C<sub>2</sub>H<sub>6</sub><sup>+</sup>), neutral radicals (H, CH, CH<sub>2</sub>, CH<sub>3</sub>, CH<sub>5</sub>) as well as the excited species (Ar<sup>\*</sup>, CH<sub>4</sub><sup>\*</sup> (2*vib.*), H(2*p*, 3*p*)). The reactions of electron impact collision and those of ions and neutral species are listed in Tables 1 and 2.

In calculations, the gas flow velocities and gas pressures obtained from the gas flow calculation are inputted into the plasma simulation as well as the gas densities and dynamic viscosities obtained from the plasma simulation are inputted back into the gas flow calculation. The calculation of gas flow is performed by a laminar flow model provided in COMSOL Multiphysics. In plasma simulations, the initial electron number density is assumed to be  $1 \times 10^{12} \text{ m}^{-3}$  and initial electron energy is 4 eV. The electron energy distribution function (EEDF) is assumed Druyvesteynian distribution

**Table 2:** The reactions of ions and neutral species included in the model.

No.	Reaction	Ref.
34	$\text{CH}_4 + \text{CH}_3^+ \rightarrow \text{CH}_4^+ + \text{CH}_3$	4
35	$\text{CH}_4 + \text{CH}_3^+ \rightarrow \text{C}_2\text{H}_5^+ + \text{H}_2$	4
36	$\text{CH}_4 + \text{CH}_4^+ \rightarrow \text{CH}_5^+ + \text{CH}_3$	4
37	$\text{H}_2 + \text{CH}_4^+ \rightarrow \text{CH}_5^+ + \text{H}$	4
38	$\text{C}_2\text{H}_6 + \text{CH}_5^+ \rightarrow \text{C}_2\text{H}_5^+ + \text{CH}_4 + \text{H}_2$	4
39	$\text{CH}_4 + \text{Ar}^+ \rightarrow \text{CH}_3^+ + \text{H} + \text{Ar}$	7
40	$\text{H}_2 + \text{Ar}^+ \rightarrow \text{ArH}^+ + \text{H}$	7
41	$\text{H}_2 + \text{Ar}^+ \rightarrow \text{Ar} + \text{H}_2^+$	7
42	$\text{CH}_3 + \text{CH}_3 \rightarrow \text{C}_2\text{H}_6$	3
43	$\text{CH}_3 + \text{H} \rightarrow \text{CH}_4$	3
44	$\text{C}_2\text{H}_5 + \text{H} \rightarrow \text{CH}_3 + \text{CH}_3$	3
45	$\text{C}_2\text{H}_5 + \text{CH}_3 \rightarrow \text{C}_3\text{H}_8$	3
46	$\text{CH}_2 + \text{H} \rightarrow \text{CH} + \text{H}_2$	3
47	$\text{CH} + \text{CH}_4 \rightarrow \text{C}_2\text{H}_5$	3
48	$\text{CH}_2 + \text{CH}_4 \rightarrow \text{CH}_3 + \text{CH}_3$	3
49	$\text{CH}_2 + \text{CH}_4 \rightarrow \text{C}_2\text{H}_4 + \text{H}_2$	3
50	$\text{CH}_4 + \text{CH} \rightarrow \text{C}_2\text{H}_4 + \text{H}$	3
51	$\text{CH}_3 + \text{CH}_2 \rightarrow \text{C}_2\text{H}_4 + \text{H}$	3
52	$\text{C}_2\text{H}_5 + \text{H} \rightarrow \text{C}_2\text{H}_4 + \text{H}_2$	3
53	$\text{CH}_2 + \text{CH}_2 \rightarrow \text{C}_2\text{H}_2 + \text{H}_2$	3
54	$\text{Ar}^* + \text{Ar}^* \rightarrow \text{Ar}^+ + \text{Ar} + e^-$	10
55	$\text{Ar}^* + \text{Ar} \rightarrow \text{Ar} + \text{Ar}$	10
56	$\text{Ar}^* + \text{H}_2 \rightarrow \text{Ar} + \text{H} + \text{H}$	15

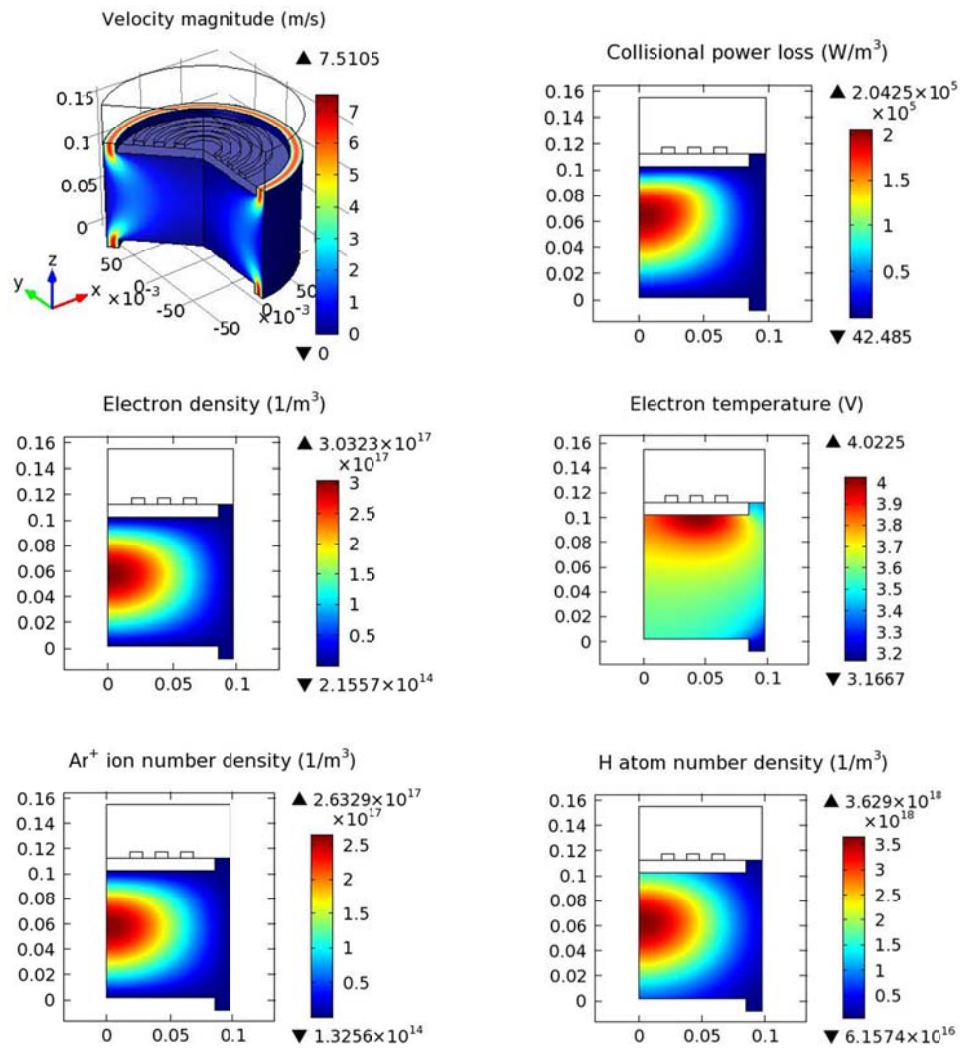


**Figure 2.** Discharge structure in a 95% Ar/5% CH<sub>4</sub> ICP plasma at a gas flow of 50 sccm.

[1,7]. The initial ion number densities are assigned by sustaining the electroneutrality. The secondary electron emission due to ion impact is set to zero and ions are considered as completely absorbed/neutralized when they arrive at the electrodes. The excited molecules and atoms are set to revert to their ground states when they contact with the walls.

### 3. Results

Figure 2 shows the calculation results for a 95% Ar/5% CH<sub>4</sub> ICP plasma at a gas flow of 50

sccm. The fast flow velocities appear around the inlet and outlet of gas flow with a maximum value of 7.51 m s<sup>-1</sup>. The maximum of electron densities arrives at 3.03×10<sup>17</sup> m<sup>-3</sup>. The electron temperature appears in the range of 3.17~4.02eV. The collisional power loss has a tendency to extend towards the inlet of gas flow from the center of plasma discharge, demonstrating that there exist strong collisions between the charged particles and inflow gas. The maximum of the densities of Ar ions arrives at 2.63×10<sup>17</sup> m<sup>-3</sup>, which is about 87% of that of electrons, governing the discharge structure. It is found that

the densities of H atoms are high, the maximum of their profiles arriving at  $3.6 \times 10^{18} \text{ m}^{-3}$ . The electron densities and electron temperatures in a function of gas flow rate for the different Ar fractions, at the maximum of their profiles, are shown in Fig. 3. The electron densities increase and electron temperatures decrease with a rise in gas flow rate for the different Ar fractions. The electron densities in a function of Ar fractions are given in Fig. 4. It is known that the electron densities rise with an increase in Ar fractions due to the decrease of collisional power losses compared with molecular states. In the present work, the effect of a small amount (5% mol) of  $\text{CH}_4$  added to Ar is found to be so large that the electron densities are greatly decreased.

The densities of ions and neutral radicals, at the maximum of their profiles, are given in Fig. 5. The effect of gas flow on  $\text{Ar}^+$  is little for the case that the Ar fractions are less than 50% and becomes important only when the Ar fractions are increased close to pure Ar. The similar effects are found for ions  $\text{CH}_5^+$ ,  $\text{C}_2\text{H}_5^+$ , and  $\text{CH}_3^+$ , which present a largest increase at a small amount (5% mol) of  $\text{CH}_4$  added to Ar. From 20 to 1000 sccm, the densities of  $\text{CH}_3^+$  ions increase one order and those of  $\text{CH}_5^+$  and  $\text{C}_2\text{H}_5^+$  increase over two orders. It is also found that at the pure  $\text{CH}_4$  discharges,  $\text{CH}_5^+$  ions are the most important ions as consistent with the previous study [3]. As the increase of Ar fractions,  $\text{C}_2\text{H}_5^+$  ions become the most important ions. The radicals  $\text{CH}_3$ ,  $\text{CH}_2$ , and  $\text{CH}$  appear high densities ( $5.5 \times 10^{17} \sim 3.5 \times 10^{18} \text{ m}^{-3}$ ) in the plasmas even in the case of 5%  $\text{CH}_4$  added to Ar. In the present work, the most major neutral radical is found to be H atom, which densities are over  $3 \times 10^{18} \text{ m}^{-3}$ . Barshilia and Vankar [5] have indicated that H atoms are a major source to deposit/etch a diamond-like carbon thin film on a wafer [5]. The present work provides an efficient method to estimate the distribution of H atoms, which would be a key to the deposition of good quality diamond thin films.

#### 4. Conclusions

This paper presents the simulation results of low-pressure inductively coupled rf plasmas in

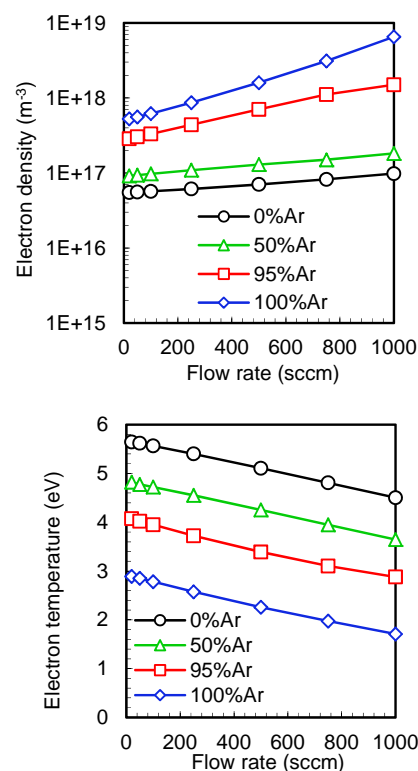


**Figure 3.** Electron densities and electron temperatures at the maximum of their profiles for the different Ar fractions at the gas flows of 20-1000 sccm.

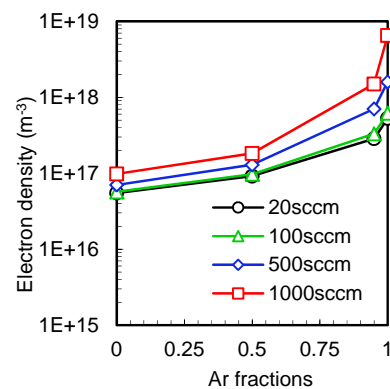


**Figure 4.** Electron densities at the maximum of their profiles for the different flow rates at the Ar fractions from 0 to 1.

$\text{Ar}/\text{CH}_4$ . The fully coupled calculation of plasma discharge and fluid dynamics is realized by COMSOL Multiphysics. It is found that the

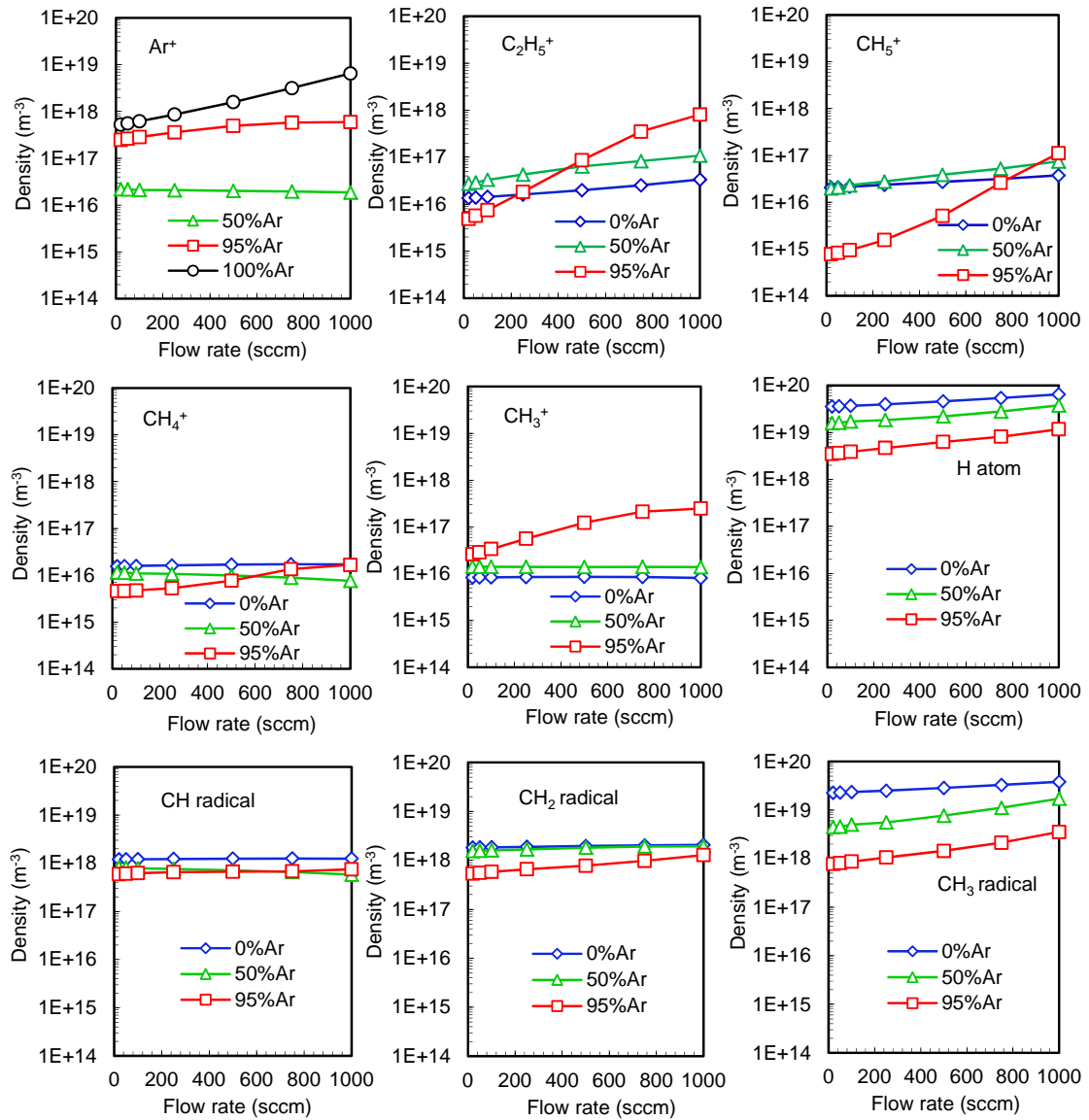


**Figure 5.** Densities of ions ( $\text{Ar}^+$ ,  $\text{C}_2\text{H}_5^+$ ,  $\text{CH}_5^+$ ,  $\text{CH}_4^+$ ,  $\text{CH}_3^+$ ) and neutral radicals (H, CH,  $\text{CH}_2$ ,  $\text{CH}_3$ ) at the maximum of their profiles for the different Ar fractions at the gas flows of 20-1000 sccm.

electron densities increase and electron temperatures decrease with a rise in gas flow rate for the different Ar fractions. The radicals  $\text{CH}_3$ ,  $\text{CH}_2$ , CH, and H appear the high densities over all the gas flow rates and different Ar fractions. The gas flows present the largest influence on plasma properties at a small amount (5%mol) of  $\text{CH}_4$  added to Ar. Results show that from 20 to 1000 sccm, the densities of  $\text{CH}_3^+$  ions increase one order and those of  $\text{CH}_5^+$  and  $\text{C}_2\text{H}_5^+$  increase

over two orders. It could be concluded that the control of gas flow rate and gas composition would be very beneficial in obtaining the deposition of good quality thin films.

## 5. References

1. K. Bera, B. Farouk, P. Vitello, "Inductively coupled radio frequency methane plasma

- simulation”, *J. Phys. D: Appl. Phys.*, **34**, 1479-1490 (2001)
2. N. Mutsukura, S. Inoue, Y. Machi, “Deposition mechanism of hydrogenated hard-carbon films in a CH<sub>4</sub> rf discharge plasma”, *J. Appl. Phys.*, **72**(1), 43-53 (1992)
  3. D. Herrebout, A. Bogaerts, M. Yan, R. Gijbels, W. Goedheer, E. Dekempeneer, “One-dimensional fluid model for an rf methane plasma of interest in deposition of diamond-like carbon layers”, *J. Appl. Phys.*, **90**(2), 570-579 (2001)
  4. A. Okita, Y. Suda, A. Ozeki, H. Sugawara, Y. Sakei, A. Oda, J. Nakamura, “Predicting the amount of carbon in carbon nanotubes grown by CH<sub>4</sub> rf plasmas”, *J. Appl. Phys.*, **99**, 014302 (2006)
  5. H.C. Barshilia, V.D. Vankar, “Concentration of atomic hydrogen in the ground state in a CH<sub>4</sub>-H<sub>2</sub> microwave plasma”, *J. Appl. Phys.*, **80**(7), 3694-3698 (1996)
  6. V. Ivanov, O. Proshina, T. Rakhimova, A. Rakhimov, “Comparison of a one-dimensional particle-in-cell-Monte Carlo model and a one-dimensional fluid model for a CH<sub>4</sub>/H<sub>2</sub> capacitively coupled radio frequency discharge”, *J. Appl. Phys.*, **91**(10), 6296-6302 (2002)
  7. I.B. Denysenko, S. Xu, J.D. Long, P.P. Rutkevych, N.A. Azarenkov, K. Ostrikov, “Inductively coupled Ar/CH<sub>4</sub>/H<sub>2</sub> plasmas for low-temperature deposition of ordered carbon nanostructures”, *J. Appl. Phys.*, **95**(5), 2713-2724 (2004)
  8. M.W. Kiehlbauch, D.B. Graves, “Inductively coupled plasmas in oxygen: Modeling and experiment”, *J. Vac. Sci. Technol. A*, **21**(3), 660-670 (2003)
  9. H. Singh, D.B. Graves, “Measurements of the electron energy distribution function in molecular gases in a shielded inductively coupled plasma”, *J. Appl. Phys.*, **88**(7), 3889-3898 (2000)
  10. COMSOL Multiphysics 4.2-Plasma Module Library Models and also <http://www.comsol.com>
  11. D.K. Davies, L.E. Kline, W.E. Bies, “Measurements of swarm parameters and derived electron collision cross sections in methane”, *J. Appl. Phys.*, **65**(9), 3311-3323 (1989)
  12. <http://www.kinema.com/download.htm>
  13. <http://www.nist.gov/pml/data/index.cfm>
  14. D.A. Alman, D.N. Ruzic, J.N. Brooks, “A hydrocarbon reaction model for low temperature hydrogen plasmas and an application to the Joint European Torus”, *Phys. Plasmas*, **7**(5), 1421-1432 (2000); *Phys. Plasmas*, **9**(2), 738-740 (2002)
  15. T. Kimura, H. Kasugai, “Properties of inductively coupled rf Ar/H<sub>2</sub> plasmas: Experiment and global model”, *J. Appl. Phys.*, **107**, 083308 (2010)

## 6. Acknowledgements

The author would like to thank Emeritus Professor K. Nanbu of Tohoku University, Japan for the helpful discussion regarding this research.